Al-Mustansiriyah Journal of Science
ISSN: 1814-635X (print) 2521-3520 (electronic)

ORIGINAL ARTICLE OPEN ACCESS

Synthesis and Characterization of Graphene Oxide for Efficient Adsorptive Removal of Hymexazol Pesticide from Aqueous Solutions: Thermodynamic, Kinetic, and Isotherm Studies

Fatima Mohammed Abdullah [a], Ahmad Hussain Ismail [a], and Ahmed Mahdi Rheima [a]

[a] Department of Chemistry, College of Science, Mustansiriyah University, Baghdad, Iraq

CORRESPONDANCE
Fatima Mohammed Abdullah
fatima1997mohammed1997@gmail.com

ARTICLE INFO
Received: September 19, 2023
Revised: December 18, 2023
Accepted: January 02, 2024
Published: June 30, 2024

ABSTRACT: ***Background:*** *Nanomaterials play a significant role in the field of water treatment due to their environment-friendly and appealing physical and chemical characteristics.* ***Objective:*** *The purpose of this research is to evaluate whether graphene oxide adsorbents can effectively remove hymexazol pesticide from an aqueous solution.* ***Methods:*** *Graphene oxide (GO) was prepared by the modified Hummer method, and it was characterized by a number characterization techniques, including XRD, Raman spectroscopy, FE-SEM, TEM, and EDX. Furthermore, the performances of the GO adsorbents for the removal of hymexazol from aqueous solution were investigated. The effect of contact time, GO dosage, initial hymexazol concentration, and temperature was carefully studied.* ***Results:*** *The kinetic experimental data were best described by the pseudo-second-order kinetic model. The equilibrium data were well fitted by the Freundlich and Langmuir isotherm models. The kinetic experimental data were best described by the pseudo-second-order kinetic model. And through the thermodynamic studies, it was found that the adsorption process of hymexazol pesticide is endothermic and spontaneous, in addition to the occurrence of adsorption and absorption together.* ***Conclusions:*** *The findings of the adsorption process demonstrated that graphene oxide is an extremely efficient adsorbent material for pesticide adsorption, owing to its large surface area and the presence of oxygen-rich groups on its surface.*

KEYWORDS: *Adsorption; Graphene Oxide; Hymexazol; Modified Hummer Method; Nanomaterial*

INTRODUCTION

Nanotechnology is an important development in contemporary science, which makes it possible to manufacture materials with unique structure, content, and size [1]–[4]. Nanotechnology-based methods have produced efficient ways and materials for the solution of many difficult problems, that prior and traditional techniques were unable to handle [5]. Nanotechnology has been applied in a variety of scientific and technological applications [6], including food industry [7], industrial processes [8], medical field [9], and environmental applications [10]. Nanomaterials also plays a significant role in the field of water treatment [11], due to the environment-friendly, appealing physical and chemical characteristics, such as increased material durability against mechanical stress or weathering, surface structure, and significant absorption, both in terms of adsorption capacity [12], [13]. A derivative of graphene, called graphene oxide (GO), has a special two-dimensional structure with -bonds connecting carbon atoms with Sp2-hybridization to form a honeycomb-lattice [14]–[16]. Functional groups including carbonyl, carboxyl, hydroxyl, and epoxy residues are abundant on its surface [17], [18]. The chemical characteristics of GO are substantially more active compared to graphene because of the existence of these oxygen-containing groups, which offer many locations for chemical reactions and ion/molecular interactions [19], [20].

GO has special properties such as high hydrophilic nature, large surface area, atomic thickness, high strength, exciting durability, and reactive sites for chemical reactions [18], [21], [22],which have

generated significant interest in different science and technology fields [23]. Due to its exceptional physicochemical features, unique surface structures, and strong affinity, graphene oxide has received extensive research as a novel adsorbent [24], [25]. GO is extremely effective in adsorbing both organic and inorganic impurities from drinking water [26]. By means of coordination π–π interactions, electrostatic interactions, H-bonding, hydrophobic interactions, and H-bonding. The oxygen-containing groups enable the binding of positive-charge-organic-molecules and metal-ions [16], [27], [28].

Clean water is a vital component of ecosystems and is critical to the survival of Earth's life. It's common knowledge that having access to clean drinking water is essential for maintaining one's health and is also a fundamental human right [29], [30].

Water pollution from pesticide residue has been growing as agricultural needs for pesticide use have expanded, posing a huge hazard to the environment [31], [32].

Pesticides are among the most harmful organic pollutants, causing major health concerns such as cancer, endocrine dysfunction, and immunological dysregulation when present in water [33]–[35]. One of the pesticides that contaminates the environment is hymexazol [36], which has been classified as a hazardous substance for humans by the European Food Safety Authority (EFSA). According to research, the liver is the major target organ upon exposure to the hymexazol pesticide. Hymexazol pesticides are particularly toxic to fish embryos, resulting in swing abnormalities, growth retardation, and heart edema [37], [38].

The aim of this research is to prepare graphene oxide by the modified Hummers method and use it as an adsorbent to remove hymexazol pesticide from aqueous solutions. The structure and morphology of the prepared graphene oxide were studied. And study the thermodynamics, isotherms, and kinetics of the adsorption process.

MATERIALS AND METHODS

Graphite powder (99.9%), Sulfuric acid (98%), hydrochloric acid, potassium permanganate (99.5%), distilled water, sodium nitrate (99%), hydrogen peroxide (30%), hymexazol (36%) SL, deionized water.

Synthesis of Graphene Oxide

According to the modified Hummers method, graphite (2 g) and $NaNO_3$ (1 g) were mixed with 100 ml of H2SO4 (98%). Und kept stirring with temperature control (≈5 °C) for 30 min. Then, 5 g of $KMnO_4$ was gradually added to the mixture and kept stirring for 5 hours. After that, 1 L of distilled water was added to the mixture. Then 30% H_2O_2 is added in a volume of 20 ml to the mixture for stopping the reaction. Following that, the product precipitate underwent centrifugation to be separated, and it was repeatedly washed with de-ionized water and 12% HCl solution. At room temperature, the dark brown product was allowed to dry overnight to produce GO [39].

Adsorption Experiment

Adsorption experiments were conducted using the hymexazol pesticide at concentrations ranging from 10 to 50 ppm. With the addition of varying amounts of the GO (0.01-0.15 g) to ten milliliters of the hymexazol pesticide solution at a particular concentration. After that, the mixture was agitated in an orbital shaker with continuous stirring at 185 rpm to complete the adsorption process for a specific time. After that, the GO was separated from the solution by centrifugation for 15 min. A UV-Vis spectrophotometer was used to determine the residual pesticide concentration at 238 nm. The amount of the adsorbed pesticide (Qe) and the removal efficiency (R%) were estimated using the equations below [39]–[41]:

$$Q_e = \frac{(C_0 - C_e)V}{M} \tag{1}$$

$$R\% = \frac{C_0 - C_0}{C_0} \times 100\% \tag{2}$$

Where is Qe is equilibrium capacity (mg/g), Co and Ce are initial and equilibrium pesticide concentration (ppm), respectively. V is volume of pesticide (l), and M is mass of GO (g).

 DOI: https://doi.org/10.23851/mjs.v35i2.1493

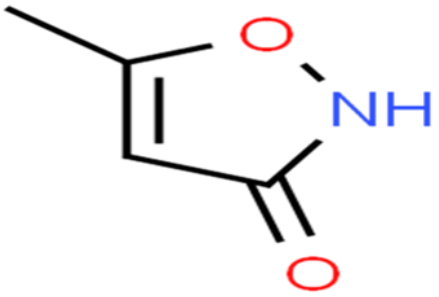

Figure 1. Chemical structure of hymexazol [42]

RESULTS AND DISCUSSION

Characterization

The crystallite size and crystal phases of synthesized GO were investigated using the XRD technique with Cu Ka radiations ($\lambda = 1.5406$ nm) in 2θ. Figure 2, shows the XRD patterns of GO in the 10-80° range. The diffraction peaks of GO were detected around $2\theta = 26^{o}$ corresponding to (002) and $2\theta = 42°$ corresponding to (100) were referred to the carbon structure in graphite. The broad peak corresponding to the (002) at $2\theta = 26°$ indicating the inclusion of oxygen functional groups during the oxidation of graphite [43].

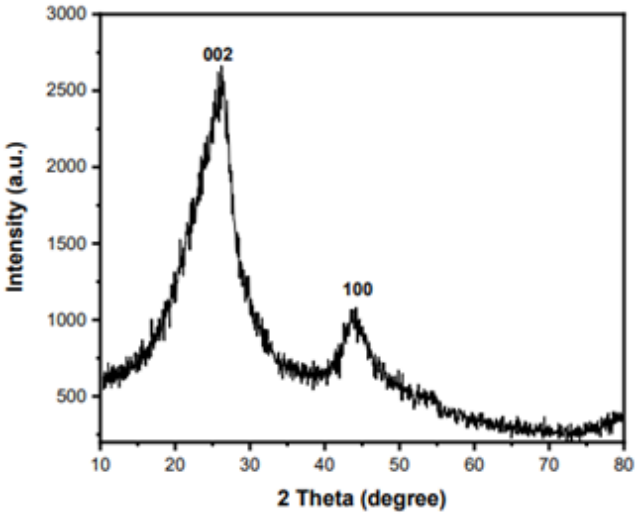

Figure 2. XRD of GO synthesis using the hummer method

Raman spectroscopy is powerful and non-destructive analytical approach. Utilized to obtain information about carbon-based material's structure and properties. [44], [45]. The G and D bands are the most commonly used characteristics of the spectrum to track changes throughout different treatments [46]. Typical Figure 3, depicts the GO Raman spectra. peaks near (1350 and 1590 cm^{-1}) could be seen in the produced GO sheets' Raman spectra. In the case of GO, the D is obtained at 1350 cm^{-1} and G peaks is at obtained 1590 cm^{-1}. The stretching of the C-C bond is attributed to the G peak, The presence of functional groups containing oxygen on graphene sheets is associated to D-peak [47], [48]. The 2D bands, which have two peaks at (2600 cm^{-1} and 2950 cm^{-1}).

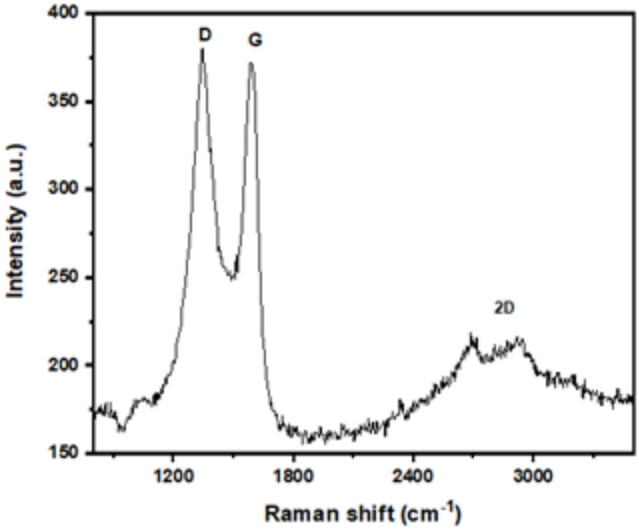

Figure 3. Raman spectra of GO

The morphology of the produced GO as determined by FE-SEM as shown in Figure 4. Where the 2D structure of GO with several thin layers was observe. This layer developed in wrinkled forms, one on top of another, this is due to graphite exfoliation that produces graphene oxide, which causes restacking and exfoliation [49].

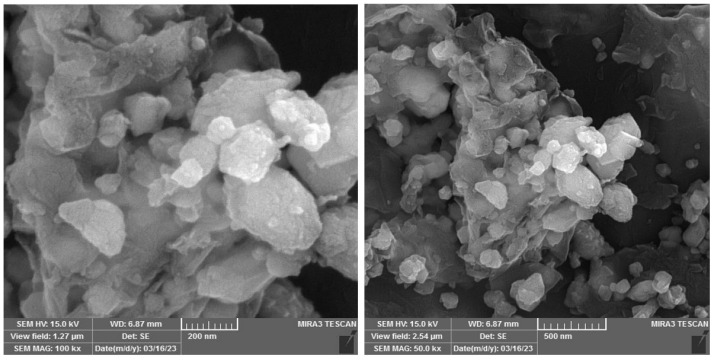

Figure 4. FESEM image of GO

The TEM image of synthesized GO shows in Figure 5, that the higher degrees of clarity signify significantly thinner films of a few layers of GO formed through stocking exfoliation. Some wrinkling of the sheets can also be observed; this is due to the presence of oxygen-rich functional groups associated with graphene sheets [50].

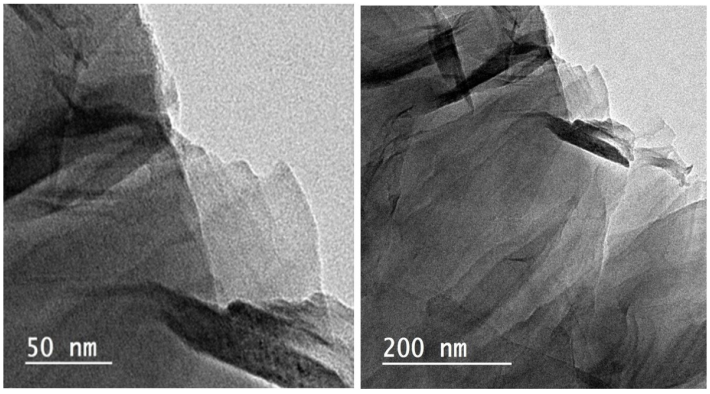

Figure 5. TEM image of GO

Through HRTEM analysis, direct information can be obtained about the atomic level of graphene oxide [51]. Figure 6, shows the finger print of prepared GO (d-spacing 0.24 nm), which belongs to the graphitic structure [52].

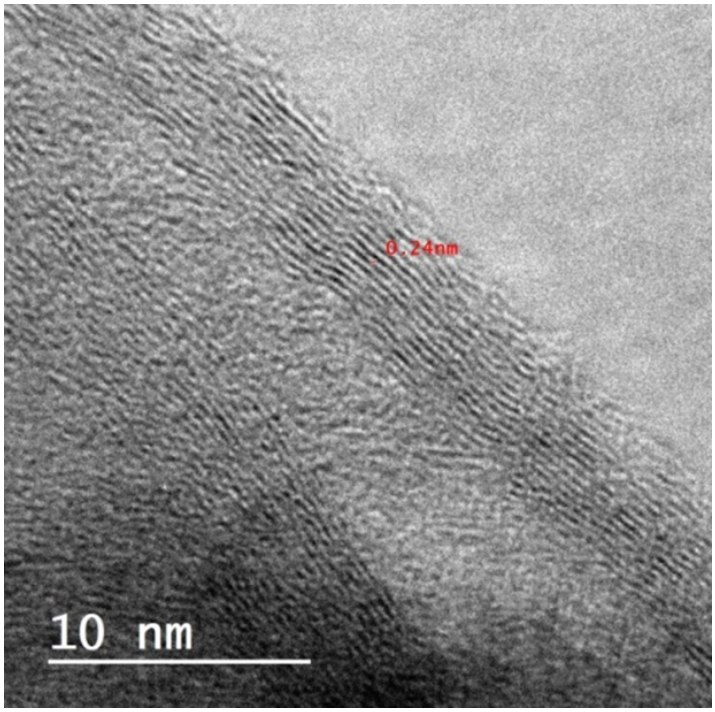

Figure 6. HRTEM of GO

EDX analysis confirmed the high purity of GO. Through Figure 7, prepared GO consists of 57.7% Carbon and 43.3% Oxygen.

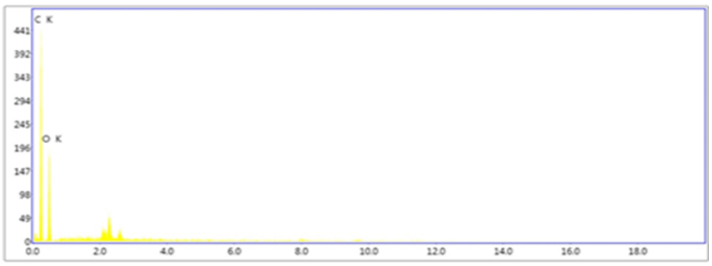

Figure 7. EDX image of GO synthesis using hummer method

Figure 8, shows the regular distribution of the O and C atoms on the GO surface, this indicating that the atoms adopt multiple places in the sample, giving a wide area for diffusion, which is one of the characteristics of nanomaterials where they are the smallest sizes and a large surface area.

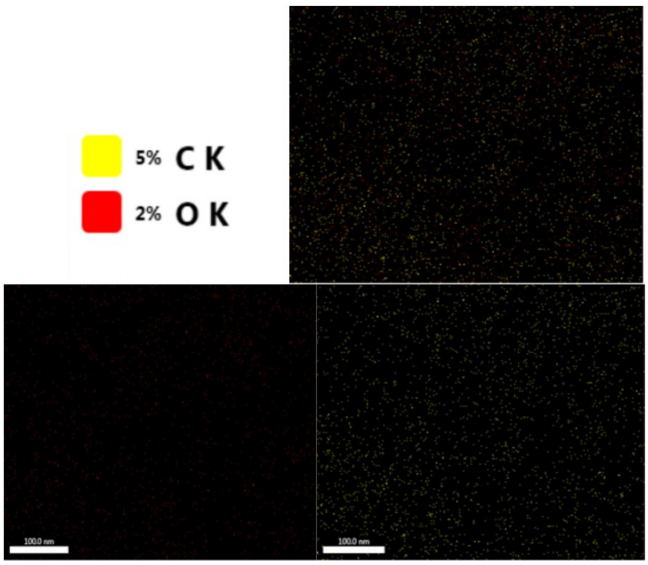

Figure 8. X-ray mapping of GO nano-sheet synthesis using the hummer method

Adsorption study

Effect of Contact Time

The effect of connect time was studied by adding 0.01 g of GO to 10 mL of hymexazol solution (50 ppm) at 25 °C with a stirring speed of 185 rpm at various intervals of time in the adsorption of hymexazol pesticide. It was observed that the removal efficiency increased directly with the increase in contact time, reaching equilibrium at 60 min. After that, the rate of the adsorption process became constant, in order to saturate the active sites with hymexazol molecules, and only a few of them are still active, so it takes a longer time to perform the adsorption process [53].

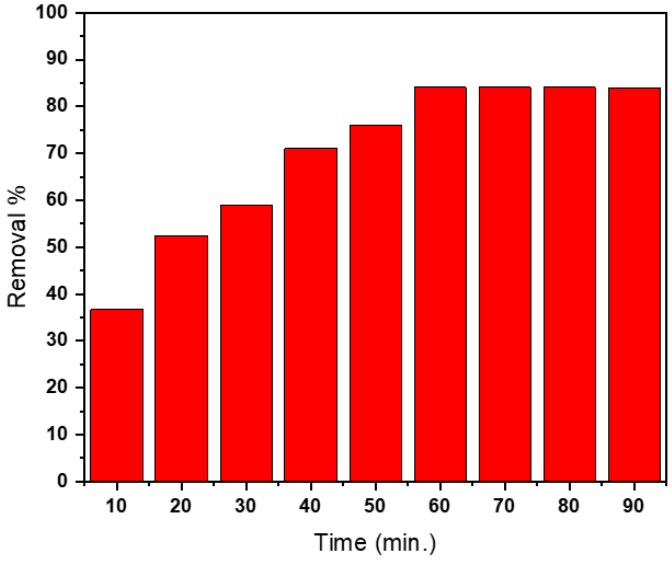

Figure 9. Effect of contact time on adsorption of hymexazol pesticide

Effect of GO Dosage

The effect of GO dosage on the pesticide adsorption was investigated by adding different amounts of GO within the range (0.01-0.15 g) to 10 ml of hymexazol pesticide solution (50 ppm). Figure 10, shows that the removal efficiency of hymexazol pesticide increased with increasing dose of GO, due

to the increase of the active sites on the GO surface [54], as a result, more hymexazol molecules were removed from the solution until total saturation was achieved.

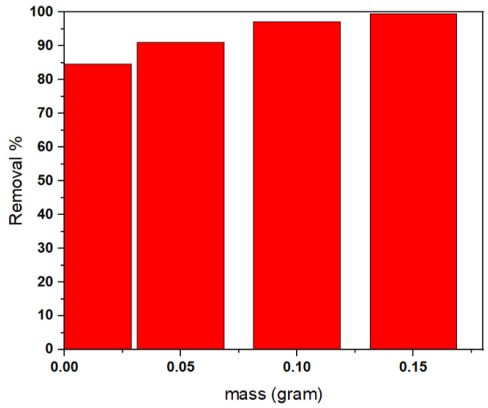

Figure 10. Effect of GO dose on adsorption of hymexazol pesticide

Effect of Temperature and Thermodynamic Parameter Calculation

These experiments were conducted at five specific temperatures, from 288 to 328 K, to investigate the temperature effect on the effectiveness of GO for the adsorption of hymexazol pesticide.

An increase in temperature leads to an increase in adsorption efficiency. This is due to an increase in both the surface energy and molecular diffusion of hymexazol pesticides on the surface of GO with the increase in adsorption temperature Adsorption efficiency increases with temperature. This is due to an increase in both the surface energy and molecular diffusion of pesticides on the surface of nanomaterials, enhanced strong binding linked the hymexazol molecules and surface of GO.

The thermodynamic parameters, including entropy change (ΔS), enthalpy change (ΔH), and Gibbs energy change (ΔG), reveal specific information about the mechanism and nature of the adsorption process. The following equations is used to determine the thermodynamic parameters [55], [56]:

$$\ln(K_e) = -\frac{\Delta H}{RT} + \frac{\Delta S}{R} \tag{3}$$

$$K_e = \frac{Q_e}{C_e} \tag{4}$$

$$\Delta G = \Delta H - T\Delta S \tag{5}$$

where Ke is an equilibrium constant, R is a gas constant (8.314 J/mole.K), and T is the temperature in Kelvin. From the slope and interception of the plots of van't Hoff, ΔH and ΔS were identified as shown in Figures 11. The S value was found to be 87.47 (J/mole.K) from the intercept, which suggests that the surface of the adsorbent becomes more random and disordered. The corresponding ΔH from the slope was 21.87 (kJ/mole), which indicated the process was endothermic. And G was determined to be -4.199 (KJ/mole), which means spontaneous adsorption.

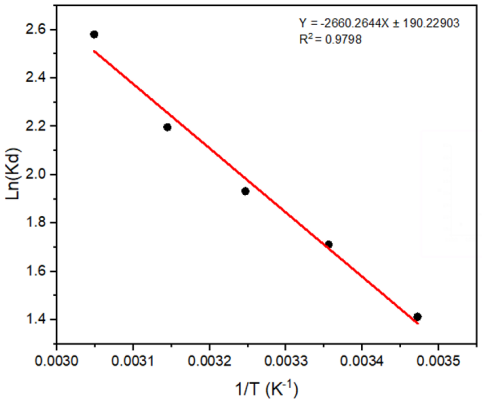

Figure 11. Van't Hoff' plot relation between $\ln(K_e)$ and $\frac{(1)}{T}$ for hymexazol adsorption

Adsorption Kinetics

The study of kinetic adsorption is very important to know the mechanism and response rate of the adsorption process [57].

The present study used two kinetic models, pseudo-first-order and pseudo-second-order models, to investigate the kinetics and controlling mechanisms of the adsorption hymexazol pesticide process. The linearized form of the pseudo-first-order model equation is generally described as [58]:

$$\ln(q_e - qt) = \ln(q_e) - k_1 t \tag{6}$$

The pseudo-second-order model equation is given as [59]:

$$\frac{1}{qt} = \frac{1}{k_2 q_e} + \frac{t}{q_e} \tag{7}$$

Where qt and qe (mg/g) amount of pesticide adsorbed at time t (min) and equilibrium (mg/g), respectively. K1 (1/min) is rate constants of pseudo-first order, and K2 (g/mg min) is rate constants of the pseudo second-order.

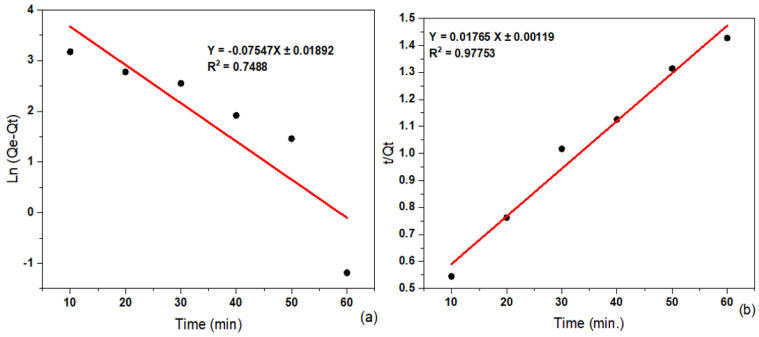

Figure 12. Kinetic of adsorption Hymexazol pesticide: (a) pseudo-first-order and (b) pseudo-second-order

Table 1. Kinetic parameters for adsorption of hymexazol pesticide

pseudo first order	**K1 (min^{-1})**	**R^2**
	0.0013	0.7488
pseudo second order	**K2 (g.mg/min)**	**R^2**
	0.0008	0.9775

A pseudo-second-order model with a high correlation coefficient (R2 > 0.9775) can accurately describe the kinetic information; this also suggests that the adsorption mechanism was improved via

chemisorption, which involves the share of electrons that take place between the adsorbent surface and the adsorbate molecular [60].

Adsorption isotherms

Adsorption data should be fit with isothermal adsorption in order to comprehend the relationship between the surface of GO and the hymexazol. In this study, both the Freundlich and Langmuir isotherm models were considered. The following equation represents to the Freundlich isotherm model [61]:

$$\log_n(Q_e) = \log_n(kf) + \frac{1}{n}\log_n(Ce) \tag{8}$$

Adsorption capacity (Kf) and adsorption intensity (n), which refer to the Freundlich constants. Kf can be found from the slope, while n is obtained from the intercept.

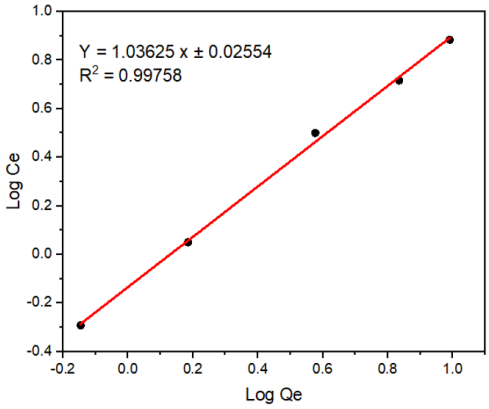

Figure 13. Freundlich isotherm for adsorption of hymexazol pesticide

The value of 1/n was determined to be 0.519, and these findings demonstrate its favorable physical adsorption [62]. Langmuir isotherm model is given by equation (9) [63]:

$$\frac{e}{q_e} = \frac{1}{(q_{max} \cdot K)} + \frac{c_e}{q_{max}} \tag{9}$$

Which q max is maximum amount of hymexazol adsorbed per gram of GO, and KL is Langmuir constant.

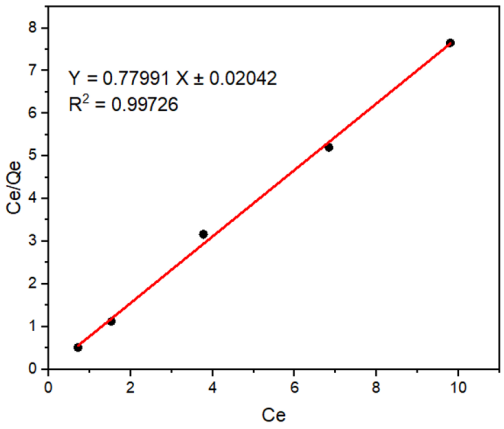

Figure 14. Langmuir isotherm for adsorption of hymexazol pesticide

Based on the correlation coefficient (R2) values, both the Freundlich and Langmuir models very closely fit the adsorption process.

A separation factor (RL) was used to determine the suitability of an adsorption process. RL is given by the following equation [64]:

$$RL = \frac{1}{1 + KL \cdot Ci} \tag{10}$$

The RL value was determined to be 0.0194, which indicates the adsorption process is favorable [65].

CONCLUSION

High-quality GO was prepared by a modified Hummer method according to the XRD, Raman spectroscopy, FESEM, TEM, and EDX characterizations. The prepared GO was used to remove the hymexazol pesticide from aqueous solutions. The findings of the adsorption process demonstrated that graphene oxide is an extremely efficient adsorbent material for pesticide adsorption, owing to its large surface area and the presence of oxygen-rich groups on its surface. The equilibrium data were well fitted by the Freundlich and Langmuir isotherm models. The calculations of the thermodynamic parameters gave the adsorption values for ΔS, ΔH, and ΔG equal to 21.87 (kJ/mole), 87.47 (J/mole), and -4.199 (KJ/mole), respectively. These results demonstrate that the adsorption was endothermic and spontaneous.

SUPPLEMENTARY MATERIAL

None.

AUTHOR CONTRIBUTIONS

Ahmed Mahdi Rheima suggested the research idea, Ahmad Hussain Ismail performed the theoretical section, and Fatima Mohammed Abdullah organized all the results and data and wrote and revised the manuscript. All authors agreed to the final version of this manuscript.

FUNDING

None.

DATA AVAILABILITY STATEMENT

None.

ACKNOWLEDGMENTS

The authors are grateful to the Department of Chemistry at the College of Science at Mustansiriyah University for providing the facilities and constant encouragement for this work.

CONFLICTS OF INTEREST

The authors declare no conflicts of interest.

REFERENCES

[1] A. M. Rheima, "Zinc oxide nanotubes: Synthesis, diagnosis and study the adsorption ability of mercury and lead ions from their aqueous solutions," *Journal of Advanced Sciences and Nanotechnology*, pp. 20–36, 2022. doi: 10.55945/joasnt.2022.1.1.20-36.

[2] A. R. Laftah, "New synthesis of bao nanoparticles using the uv-irradiation technique for removal cibacron blue dye from their aqueous solution," *Egyptian Journal of Chemistry*, p. 13, 2022. doi: 10.21608/ejchem.2022.126902.5651.

[3] B. E. Jasim, "Nickel oxide nanofibers manufactured via sol-gel method: Synthesis, characterization and use it as a photo-anode in the dye sensitized solar cell," *Digest Journal of Nanomaterials & Biostructures (DJNB)*, 2022. doi: 10.15251/DJNB.2022.171.59.

[4] A. Rheima, "Novel method to synthesis nickel oxide nanoparticles for antibacterial activity," *Iranian Journal of Physics Research*, pp. 51–55, 2020. doi: 10.47176/ijpr.20.3.38771.

[5] A. Awasthi, "Clay nano-adsorbent: Structures, applications and mechanism for water treatment," *SN Applied Sciences*, vol. 1, pp. 1–12, 2019. doi: 10.1007/s42452-019-0858-9.

[6] S. Husain, "Emerging trends in advanced translational applications of silver nanoparticles: A progressing dawn of nanotechnology," *Journal of Functional Biomaterials*, vol. 14, no. 1, p. 47, 2023. doi: 10.3390/jfb14010047.

[7] G. Vijayakumar, "Detection of food toxins, pathogens, and microorganisms using nanotechnology-based sensors," in *Nanotechnology Applications for Food Safety and Quality Monitoring*. 2023, pp. 155–170. doi: 10.1016/B978-0-323-85791-8.00022-7.

[8] S. Malik, "Nanotechnology: A revolution in modern industry," *Molecules*, vol. 28, no. 2, p. 661, 2023. doi: 10.3390/molecules28020661.

[9] L. Inbathamizh, "Nanotechnology: Ethical impacts, health issues, and safety issues," in *Modern Nanotechnology: Volume 2: Green Synthesis, Sustainable Energy and Impacts*. 2023, pp. 455–477. doi: 10.1007/978-3-031-31104-8_20.

[10] P. Biswas, "Advanced implications of nanotechnology in disease control and environmental perspectives," *Biomedicine & Pharmacotherapy*, vol. 158, p. 114 172, 2023. doi: 10.1016/j.biopha.2022.114172.

[11] K. Neeti, "The role of green nanomaterials as effective adsorbents and applications in wastewater treatment," *Materials Today: Proceedings*, vol. 77, pp. 269–272, 2023. doi: 10.1016/j.matpr.2022.11.300.

[12] R. Kumar, *Advanced Functional Nanoparticles" Boon or Bane" for Environment Remediation Applications: Combating Environmental Issues*. 2023. doi: 10.1007/978-3-031-24416-2.

[13] H. Hu, "Physicochemical technologies for hrps and risk control," in 2020, pp. 169–207. doi: 10.1016/B978-0-12-816448-8.00008-3.

[14] F. Tunioli, "Adsorption of emerging contaminants by graphene related materials and their alginate composite hydrogels," *Journal of Environmental Chemical Engineering*, p. 109 566, 2023. doi: 10.1016/j.jece.2023.109566.

[15] U. Rajaji, "A sonochemical synthesis of srtio3 supported n-doped graphene oxide as a highly efficient electrocatalyst for electrochemical reduction of a chemotherapeutic drug," *Ultrasonics Sonochemistry*, p. 106 293, 2023. doi: 10.1016/j.ultsonch.2023.106293.

[16] L. Liang, "In situ synthesis of a go/cofs composite with enhanced adsorption performance for organic pollutants in water," *Environmental Science: Nano*, pp. 554–567, 2022. doi: 10.1039/D1EN01015H.

[17] H. Jafarian, "Synthesis of heterogeneous metal organic framework-graphene oxide nanocomposite membranes for water treatment," *Chemical Engineering Journal*, p. 140 851, 2023. doi: 10.1016/j.cej.2022.140851.

[18] V. Palmieri, "Graphene oxide-mediated copper reduction allows comparative evaluation of oxygenated reactive residues exposure on the materials surface in a simple one-step method," *Applied Surface Science*, p. 156 312, 2023. doi: 10.1016/j.apsusc.2022.156315.

[19] F. Jia, "Advances in graphene oxide membranes for water treatment," *Nano Research*, pp. 6636–6654, 2022. doi: 10.1007/s12274-022-4273-y.

[20] Y. Li, "Tailoring the physicochemical and geometric properties of two-dimensional graphene membranes for aqueous separation," *Desalination*, vol. 530, p. 115 621, 2022. doi: 10.1016/j.desal.2022.115621.

[21] Y. Rezaeipour, "The anticancer properties of metal-organic frameworks and their heterogeneous nanocomposites," *Biomaterials Advances*, p. 213 013, 2022. doi: 10.1016/j.bioadv.2022.213013.

[22] K. Chen, "Graphene oxide bulk material reinforced by heterophase platelets with multiscale interface crosslinking," *Nature Materials*, pp. 1121–1129, 2022. doi: 10.1038/s41563-022-01292-4.

[23] D. J. Joshi, "Surface modifications and analytical applications of graphene oxide: A review," *TrAC Trends in Analytical Chemistry*, p. 116 448, 2021. doi: 10.1016/j.trac.2021.116448.

[24] Y. A. B. Neolaka, "The adsorption of cr (vi) from water samples using graphene oxide-magnetic (go-fe3o4) synthesized from natural cellulose-based graphite (kusambi wood or schleichera oleosa): Study of kinetics, isotherms and thermodynamics," *Journal of Materials Research and Technology*, vol. 9, no. 3, pp. 6544–6556, 2020. doi: 10.1016/j.jmrt.2020.04.040.

[25] R. H. Krishna, "Carbon nanotubes and graphene-based materials for adsorptive removal of metal ions–a review on surface functionalization and related adsorption mechanism," *Applied Surface Science Advances*, vol. 13, p. 100 431, 2023. doi: 10.1016/j.apsadv.2023.100431.

[26] B. F. M. L. Gomes, "Synthesis and application of graphene oxide as a nanoadsorbent to remove cd (ii) and pb (ii) from water: Adsorption equilibrium, kinetics, and regeneration," *Environmental Science and Pollution Research*, pp. 17 358–17 372, 2022. doi: 10.1007/s11356-021-16943-3.

[27] N. Jahan, "A comparative study on sorption behavior of graphene oxide and reduced graphene oxide towards methylene blue," *Case Studies in Chemical and Environmental Engineering*, p. 100 239, doi: 10.1016/j.cscee.2021.100239.

[28] R. G. Abaszade, "Synthesis and analysis of flakes graphene oxide," *Journal of Optoelectronic and Biomedical Materials*, pp. 107–114, 2022. doi: 10.15251/JOBM.2022.143.107.

[29] A. Verma, "Application of wastewater in agriculture: Benefits and detriments," in *River Conservation and Water Resource Management*. 2023, pp. 53–75. doi: 10.1007/978-981-99-2605-3_4.

[30] I. El-Nahhal, "Pesticide residues in drinking water, their potential risk to human health and removal options," *Journal of Environmental Management*, p. 113 611, 2021. doi: 10.1016/j.jenvman.2021.113611.

[31] M. S. Nazir, "Remediation of pesticide in water," in *Sustainable Agriculture Reviews 47*. 2021, pp. 271–307. doi: 10.1007/978-3-030-54712-7_8.

[32] N. Dhankhar, "Impact of increasing pesticides and fertilizers on human health: A review," *Materials Today: Proceedings*, 2023. doi: 10.1016/j.matpr.2023.03.766.

[33] C. Panis, "Widespread pesticide contamination of drinking water and impact on cancer risk in brazil," *Environment International*, p. 107 321, 2022. doi: 10.1016/j.envint.2022.107321.

[34] S. Boulkhessaim, "Emerging trends in the remediation of persistent organic pollutants using nanomaterials and related processes: A review," *Nanomaterials*, p. 2148, 2022. doi: 10.3390/nano12132148.

[35] S. Singh, "Pesticides in water," in *Handbook of water purity and quality*. 2021, pp. 231–253. doi: 10.1016/B978-0-12-821057-4.00004-5.

[36] A. Yousfi, "Bifenthrine & hymexazol toxic effects on helix aspersa and the evaluation of the protective effect of orange essential oils," *Annals of the Romanian Society for Cell Biology*, vol. 26, no. 01, pp. 3270–3284, 2022.

[37] E. I. Hassanen, "A comprehensive study on the mechanistic way of hexaflumuron and hymexazol induced neurobehavioral toxicity in rats," *Neurochemical Research*, vol. 47, no. 10, pp. 3051–3062, 2022. doi: 10.1007/s11064-022-03654-5.

[38] N. H. Hassan, "The potential mechanism underlying the hepatorenal toxicity induced by hymexazol in rats and the role of nf- b signaling pathway," *Journal of Biochemical and Molecular Toxicology*, e23304, 2023. doi: 10.1002/jbt.23304.

[39] F. Mohammed, "Effective removal of hymexazol pesticide from polluted water using cadmium oxide nanoparticles prepared by photolysis methods: Thermodynamic, kinetic, and isothermal studies," *Journal of Wildlife and Biodiversity*, vol. 7, no. Special Issue, pp. 586–600, 2023.

[40] P. Chen, "Selective removal of heavy metals by zr-based mofs in wastewater: New acid and amino functionalization strategy," *Journal of Environmental Sciences*, pp. 268–280, 2023. doi: 10.1016/j.jes.2021.10.010.

[41] M. A. Báez-Sañudo, "Assessment of residuality of hymexazol in strawberry (fragaria× ananassa) crop by a modified quechers method and liquid chromatography tandem-mass spectrometry," *Agronomy*, vol. 12, no. 12, p. 3110, 2022. doi: 10.3390/agronomy12123110.

[42] K. D. Khalil, "Fabrication of dye-sensitized solar cells and synthesis of cunio2 nanostructures using a photo-irradiation technique," *Polymers*, p. 2827, 2022. doi: 10.22052/JNS.2022.01.014.

[43] X. Xu, "Biosynthesis of sorafenib coated graphene nanosheets for the treatment of gastric cancer in patients in nursing care," *Journal of Photochemistry and Photobiology B: Biology*, vol. 191, pp. 1–5, 2019. doi: 10.1016/j.jphotobiol.2018.11.013.

[44] Z. Li, "Raman spectroscopy of carbon materials and their composites: Graphene, nanotubes and fibres," *Progress in Materials Science*, p. 101 089, 2023. doi: 10.1016/j.pmatsci.2023.101089.

[45] S.-h. Urashima, "Non-destructive estimation of the cation composition of natural carbonates by micro-raman spectroscopy," *Analytica Chimica Acta*, p. 340 798, 2023. doi: 10.1016/j.aca.2023.340798.

[46] S. Farah, "Comparison of thermally and chemically reduced graphene oxides by thermal analysis and raman spectroscopy," *Journal of Thermal Analysis and Calorimetry*, pp. 331–337, 2020. doi: 10.1007/s10973-020-09719-3.

[47] S. Bidmeshkipour, "Graphene nanopores in broadband wide-angle optical cavity resonance absorbers," *Surfaces and Interfaces*, p. 101 956, 2022. doi: 10.1016/j.surfin.2022.101956.

[48] T. Bandara, "An electrochemical route to exfoliate vein graphite into graphene with black tea," *Materials Chemistry and Physics*, p. 126 450, 2022. doi: 10.1016/j.matchemphys.2022.126450.

[49] E. Jaafar, "Study on morphological, optical and electrical properties of graphene oxide (go) and reduced graphene oxide (rgo)," in *Materials Science Forum*. 2018. doi: 10.4028/www.scientific.net/MSF.917.112.

[50] N. S. Suhaimin, "The evolution of oxygen-functional groups of graphene oxide as a function of oxidation degree," *Materials Chemistry and Physics*, p. 125 629, 2022. doi: 10.1016/j.matchemphys.2021.125629.

[51] X. Wang, "Quantifying orientation and curvature in hrtem lattice fringe micrographs of naturally thermally altered coals: New insights from a structural evolution perspective," *Fuel*, p. 122 180, 2022. doi: 10.1016/j.fuel.2021.122180.

[52] S. Deng, "In vivo toxicity assessment of four types of graphene quantum dots (gqds) using mrna sequencing," *Toxicology Letters*, pp. 55–66, 2022. doi: 10.1016/j.toxlet.2022.05.006.

[53] Y. E. Hassen, "Dodonaea angustifolia extract-assisted green synthesis of the cu2o/al2o3 nanocomposite for adsorption of cd(ii) from water," *ACS Omega*, vol. 8, no. 19, pp. 17 209–17 219, 2023. doi: 10.1021/acsomega.3c01609.

[54] P. Sikarwar, "Adsorptive denitrogenation of indole from model fuel oil over co-mac: Adsorption mechanisms and competitive adsorption," *Journal of the Indian Chemical Society*, p. 100 801, 2023. doi: 10.1016/j.jics.2022.100801.

[55] X. Qi, "Recent advances in polysaccharide-based adsorbents for wastewater treatment," *Journal of Cleaner Production*, p. 128 221, 2021. doi: 10.1016/j.jclepro.2021.128221.

[56] T. A. Aragaw, "A comparative study of acidic, basic, and reactive dyes adsorption from aqueous solution onto kaolin adsorbent: Effect of operating parameters, isotherms, kinetics, and thermodynamics," *Emerging Contaminants*, pp. 59–74, 2022. doi: 10.1016/j.emcon.2022.01.002.

[57] Z. R. Zair, "Optimization, equilibrium, kinetics and thermodynamic study of congo red dye adsorption from aqueous solutions using iraqi porcelanite rocks," *Heat and Mass Transfer*, vol. 58, no. 8, pp. 1393–1410, 2022. doi: 10.1007/s00231-022-03182-6.

[58] N. Ahadi, "Facile synthesis of hierarchically structured mil-53 (al) with superior properties using an environmentally-friendly ultrasonic method for separating lead ions from aqueous solutions," *Scientific Reports*, pp. 1–17, 2022. doi: 10.1038/s41598-022-06518-8.

[59] H. S. Alhares, "Sunflower husks coated with copper oxide nanoparticles for reactive blue 49 and reactive red 195 removals: Adsorption mechanisms, thermodynamic, kinetic, and isotherm studies," *Water, Air, & Soil Pollution*, vol. 1, no. 35, p. 234, 2023. doi: 10.1007/s11270-022-06033-6.

[60] J. N. Wekoye, "Kinetic and equilibrium studies of congo red dye adsorption on cabbage waste powder," *Environmental Chemistry and Ecotoxicology*, vol. 2, pp. 24–31, 2020. doi: 10.1016/j.enceco.2020.01.004.

[61] M. A. Al-Ghouti, "Guidelines for the use and interpretation of adsorption isotherm models: A review," *Journal of hazardous materials*, p. 122 383, 2020. doi: 10.1016/j.jhazmat.2020.122383.

[62] M. A. Al-Ghouti, "Mechanistic understanding of the adsorption and thermodynamic aspects of cationic methylene blue dye onto cellulosic olive stones biomass from wastewater," *Scientific Reports*, vol. 10, no. 1, pp. 1–18, 2020. doi: 10.1038/s41598-020-72996-3.

[63] H. Patel, "Comparison of batch and fixed bed column adsorption: A critical review," *International Journal of Environmental Science and Technology*, pp. 10 409–10 426, 2022. doi: 10.1007/s13762-021-03492-y.

[64] C.-K. How, "Adsorption properties of -carotene on mesoporous carbon-coated honeycomb monolith: Kinetics, thermodynamics, and regeneration studies," *Korean Journal of Chemical Engineering*, vol. 39, no. 11, pp. 3109–3120, 2022. doi: 10.1007/s11814-022-1220-2.

[65] I. Maamoun, "Insights into kinetics, isotherms and thermodynamics of phosphorus sorption onto nanoscale zero-valent iron," *Journal of Molecular Liquids*, vol. 238, p. 115 402, 2021. doi: 10.1016/j.molliq.2021.115402.